Elimination of malachite green by modified Fenton like process. Application of Box Behnken design

Salima BENDEBANE[1*], Hawa BENDEBANE[2], Farida BENDEBANE[2], Fadhel Ismail[2]

[1]National Higher School of Technology and Engineering, Laboratory L3M, 23005, Annaba, Algeria,

[2] Laboratory LOMOP, Badji Mokhtar- Annaba University, BP 12 Annaba-Algeria

*Corresponding Authors: Salima BENDEBANE

E-mail: s.bendebane@ensti-annaba.dz , tel: +213 664 600 534

Graphical abstract

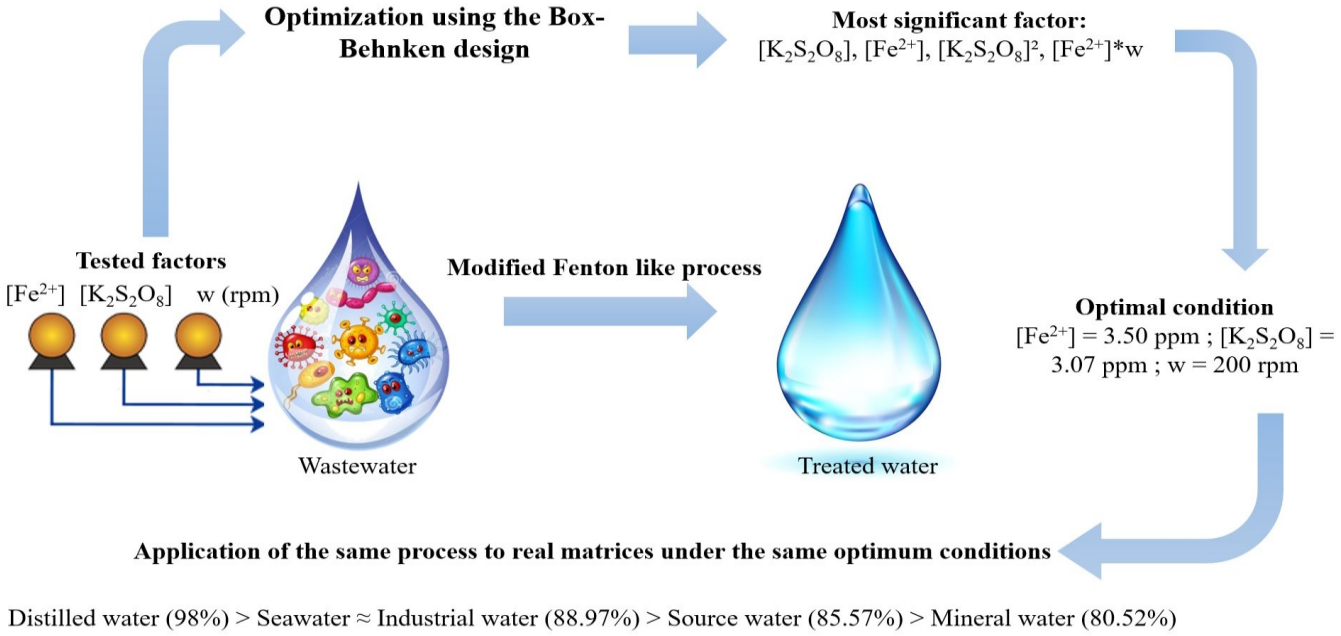

ACCEPTED MANUSCRIPT

ABSTRACT

The aim of this work was to investigate an advanced oxidation process for removing malachite green from aqueous solutions using a modified Fenton-like process. An experimental Box-Behnken design was applied to determine the optimal conditions by examining the effects of catalyst concentration ([Fe^{2+}]), oxidant concentration ([$K_2S_2O_8$]), and stirring speed. The analysis of variance (ANOVA) indicated that oxidant concentration was the most significant factor, with a p-value of 0.001, while catalyst concentration, the quadratic term of the oxidant, and the interaction between catalyst concentration and stirring speed were also significant. The optimal conditions for maximum dye removal were found to be a catalyst concentration of 3.5 ppm, an oxidant concentration of 3.07 ppm, and a stirring speed of 200 rpm, achieving a theoretical degradation yield of 100% and an experimental yield of 98%. This agreement validates the model and the importance of the optimized parameters. Additionally, degradation kinetics studies in various natural waters revealed that oxidation efficiency followed this order: Distilled water (98%) > Seawater ≈ Industrial water (88.97%) > Source water (85.57%) > Mineral water (80.52%).

Keywords: Modified Fenton oxidation, Water treatment, Box-Behnken design, Homogeneous catalysis optimization, degradation kinetics, real matrix.

ACCEPTED MANUSCRIPT

1. Introduction

With the growth of humanity, science, and technology, our world is reaching new horizons, but the cost we'll be paying soon is bound to be too high. Environmental disorder, with a major pollution problem, is among the consequences of this rapid growth. Apart from other needs, the water demand has increased enormously with the agricultural, industrial, and domestic sectors consuming 70, 22, and 8% of the available freshwater respectively, resulting in large quantities of wastewater containing several pollutants (Gupt et al. 2009, Ali Akbar et al. 2017, Karimipour et al. 2021, Azizpour et al. 2024). Once dissolved in water, they can be difficult to treat, as dyes have a synthetic origin and a complex molecular structure that makes them more stable and difficult to biodegrade (Forgacs et al. 2004, Rai et al. 2005, Jalilzadeh et al. 2014, Shobirynia et al. 2024, Brati et al. 2024). They can therefore be a risk factor for our health and a nuisance for our environment, and it is necessary to limit these pollutants as much as possible by setting up a suitable treatment method, such as a decolorization unit.

There are several physical, chemical, and biological methods for treating and decolorizing polluted effluents, such as coagulation and flocculation (Wu et al. 2015, Lee et al.2006, Zonoozi et al.2009, Zahrim et al. 2013, Souhaimi et al. 2011), membrane filtration (Jiraratananon et al. 2000, Koyuncu et al. 2002), chemical oxidation (Liu et al 2006, Ghodbane et al. 2014, Shokri et al. 2020, Nemati et al. 2024), extraction (Bendebane et al. 2016), ozonation (Lee et al. 2006, Baban et al 2010), ion exchange and electrochemical methods (Soloman et al 2009, Bahadir et al. 2008), and adsorption, etc. (Rangabhashiyam et al. 2013, Gashtasbi et al. 2017, Bendebane et al. 2021).

In recent decades, much research has focused on a new class of oxidation techniques for dyes.

This work is mainly based on the application of the modified Fenten-like process experimental design, the aim of which is to improve dye removal efficiency.

Indeed, we first studied the oxidation of malachite green by the modified Fenton-like process ($K_2S_2O_8/SO_4^{-\circ}$ system) by showing the influence of some experimental parameters on the degradation yield.

ACCEPTED MANUSCRIPT

The reactions of persulfate ions with various inorganic compounds have been extensively studied (Ivanov et al 2000), and sulfate radicals are more powerful oxidants than hydroxyl and the thermodynamics of transition metal-oxidant coupling (Anipistakis et al. 2003, Anipistakis et al. 2004), as they are more selective for oxidation (electron transfer). Hydroxyl radicals can also react rapidly through hydrogen elimination and addition, a fact also highlighted by our observation. secondly, we describe the oxidation kinetics of malachite green in a real matrix using different types of water.

2. Materials and methods

2.1. Materials

Malachite green ($C_{52}H_{56}N_4O_{12}$), Iron (II) sulfate heptahydrate (purity 99%, $FeSO_4 .7H_2O$), and sulfuric acid (purity 96-98%, H_2SO_4) were purchased from Sigma Aldrich, Potassium persulfate (purity 30%, $K_2S_2O_8$) was purchased from Biochem Chemopharma. All the solutions used in the experiments were prepared with distilled water at pH was regulated using H_2SO_4 (1 M).

2.2. Experimental procedures and analysis

The study of the degradation of malachite green by potassium persulfate ($K_2S_2O_8$) was carried out in a discontinuous, perfectly stirred and thermostated reactor shown in Figure 1.

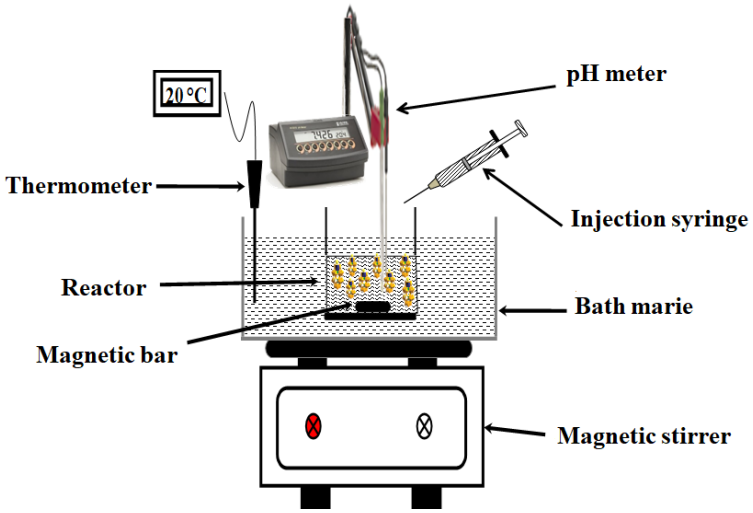

Figure 1. Experimental set-up

ACCEPTED MANUSCRIPT

The reactor is first charged with 100 mL of a 10 ppm solution of malachite green. The pH of the reaction medium is adjusted to 3 using a few drops of sulfuric acid (H_2SO_4, 98% purity). The solution is then stirred for several minutes to ensure optimum homogenization. Subsequently, a determined volume of $FeSO_4$ solution is added, followed by the introduction of a volume of $K_2S_2O_8$ solution at the specified concentration. The mixture thus prepared is subjected to controlled stirring by a magnetic stirrer, at the prescribed speed as indicated in Table 1, while maintaining the system temperature at 20°C. The oxidation reaction starts as soon as the oxidant is added. To monitor reaction kinetics, a sample is taken after one hour of reaction. The samples are then analyzed by UV-visible spectrophotometry to quantify the species in solution. The malachite green removal yield is then calculated from the following equation:

$$Y\ (\%) = \left[1 - \frac{[\mathrm{MG}]_f}{[\mathrm{MG}]_0}\right] \times 100 \qquad (1)$$

Where: $[MG]_0$ the initial concentration of dye (mg/L) ;

$[VM]_f$ the final concentration (at equilibrium) of dye (mg/L) ;

Y (%): removal efficiency of MG.

In this study, operating conditions were optimized to maximize the degradation yield of malachite green dye by applying response surface methodology (RSM), using a Box-Behnken design (BBD). Three independent variables were selected for the study: catalyst concentration [Fe^{2+}], oxidant concentration [$K_2S_2O_8$], and stirring speed, while the other operating parameters were kept constant. The persulfate ion ($S_2O_8^{2-}$) was used as the main oxidant, being one of the strongest oxidizing agents in aqueous solution, with a standard potential of 2.01 V/ENH. This potential, which is higher than that of hydrogen peroxide (H_2O_2, E°=1.78 V/ENH), gives the persulfate increased efficacy. However, to optimize its effectiveness, persulfate must be activated in the presence of catalysts, leading to the formation of the sulfate radical ($SO_4^{\cdot-}$), an even more powerful oxidant with a high oxidation potential (E° = 2.6 V/ENH) (Liang et al. 2003, Liang et al. 2008, Zhao et al. 2013).

ACCEPTED MANUSCRIPT

Table 1 summarizes the factors studied and their respective levels. Statistical analysis of the experimental data was carried out using MINITAB 18 software.

Table 1. Factors and domains studied.

Factors	**Units**	**Levels**		
		Low (-1)	**Medium (0)**	**High (+1)**
[Fe^{2+}]	ppm	2	3.5	5
[$K_2S_2O_8$]	ppm	2	6	10
W	rpm	200	300	400

3. Results and Discussion

3.1. Results

In the first part of this article, the removal of malachite green (MG) was studied from aqueous solutions prepared with distilled water, using the Box-Behnken design (BBD). The matrix presented in Table 2 combines the three factors varying according to this experimental design.

Table 2. Experiment matrix for MG degradation

Try	**[Fe^{2+}](ppm)**	**[$K_2S_2O_8$] (ppm)**	**w(rpm)**	**$Y_{exp.}$(%)**	**$Y_{th.}$ (%)**
1	3.5	6	30	96.02	96.12
2	3.5	10	40	96.57	90.39
3	2.0	2	30	48.00	54.98
4	3.5	2	20	40.71	46.88
5	3.5	6	30	96.15	96.13
6	2.0	6	20	96.27	83.11
7	3.5	2	40	38.82	28.33

ACCEPTED MANUSCRIPT

8	5.0	6	20	93.29	89.78
9	2.0	6	40	97.00	100
10	3.5	10	20	96.39	100
11	5.0	2	30	9.88	7.22
12	5.0	10	30	94.75	87.76
13	3.5	6	30	96.21	96.13
14	2.0	10	30	93.84	96.50
15	5.0	6	40	24.17	37.33

3.1.1 ANOVA

Table 3 of the analysis of variance shows that the oxidant [$K_2S_2O_8$] is a highly significant parameter for the degradation of malachite green, with a probability value of 0.001. The catalyst [Fe^{2+}], the oxidant squared ([$K_2S_2O_8$])^2 and the interaction [Fe^{2+}]*w are also significant for the degradation of MG, with a probability value of 0.001. The catalyst [Fe^{2+}], the oxidant squared ([$K_2S_2O_8$])^2 and the interaction [Fe^{2+}]*w are also significant for MG degradation, with P values of 0.024, 0.019 and 0.038 respectively.

Table 3. ANOVA results according to Box-Behnken design

Source	**DL**	**P value**
Model	9	0.011
Linear	3	**0.003**
[Fe^{2+}]	1	**0.024**
[$K_2S_2O_8$]	1	**0.001**
w	1	0.104
Square	3	0.061
[Fe^{2+}]*[Fe^{2+}]	1	0.113

ACCEPTED MANUSCRIPT

$[K_2S_2O_8]$*$[K_2S_2O_8]$	1	**0.019**
w*w	1	0.400
2-factor interaction	3	0.109
$[Fe^{2+}]$*$[K_2S_2O_8]$	1	0.179
$[Fe^{2+}]$*w	1	**0.038**
$[K_2S_2O_8]$*w	1	0.937
Error	5	
Inadequacy of fit	3	0.000
Pure error	2	
Total	14	

119

120 According to Table 4, the factors that positively influence malachite green degradation are the
121 oxidant, the $[Fe^{2+}]$*$[K_2S_2O_8]$ interaction, and the $[K_2S_2O_8]$*w interaction. On the other hand, the other
122 factors studied have a negative effect on this phenomenon

123 **Table 4.** Box-Behnken coefficients

Termes	**Coeff**	**Coef ErT**	**T value**	**P value**
Constant	96.13	7.21	13.34	0.000
$[Fe^{2+}]$	-14.13	4.41	-3.20	**0.024**
$[K_2S_2O_8]$	30.52	4.41	6.91	**0.001**
W	-8.76	4.41	-1.98	0.104
$[Fe^{2+}]$*$[Fe^{2+}]$	-12.47	6.50	-1.92	0.113
$[K_2S_2O_8]$*$[K_2S_2O_8]$	-22.03	6.50	-3.39	**0.019**
w*w	-5.97	6.50	-0.92	0.400
$[Fe^{2+}]$*$[K_2S_2O_8]$	9.76	6.24	1.56	0.179

ACCEPTED MANUSCRIPT

$[Fe^{2+}]*w$	-17.46	6.24	-2.80	**0.038**
$[K_2S_2O_8]*w$	0.52	6.24	0.08	0.937

124

125

126 *3.1.2. Histogram of residual values*

127 Figure 2 shows the histogram of residual values for the degadation yield of malachite green. From
128 this figure, we can see that the histogram follows a bell-shaped curve. This means that the residual
129 values are almost normally distributed. We can also see that the histogram values are highly
130 symmetrical, so the residual values are probably normally distributed.

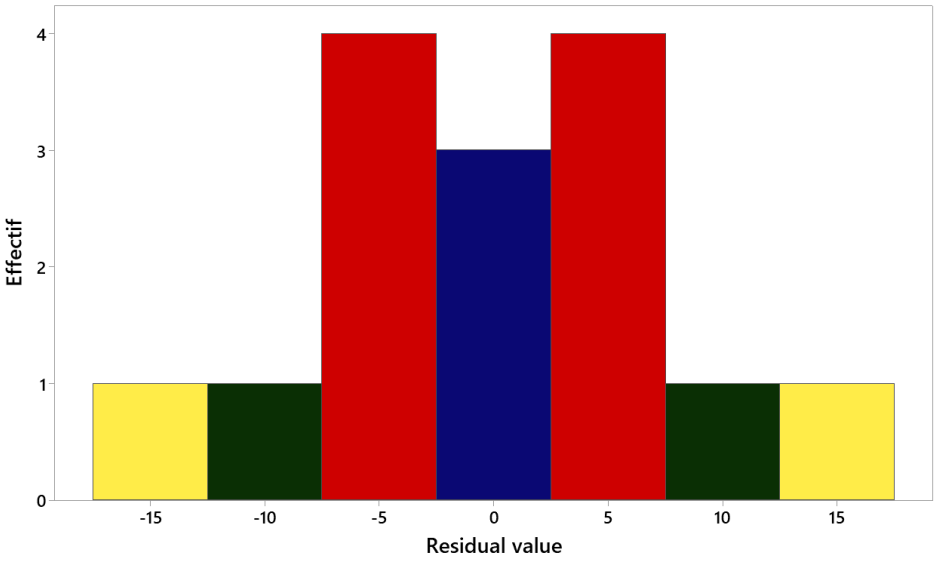

131

132 **Figure 2.** Histogram of residual values for Malachite Green degradation yield

133 *3.1.3. Main effects of the factors*

134 From Figure 4, a decrease in dye degradation yield was observed as a function of increasing Fe(II)
135 concentration as well as increasing stirring speed. For the $[Fe^{2+}]$ catalyst, the yield decreased from
136 83.78% at 2 ppm to 55.52% at 5 ppm. Similarly, agitation speed reduces yield, from 81.66% at 200
137 rpm to 64.14% at 400 rpm. On the other hand, increasing oxidant concentration has a positive effect
138 on malachite green degradation yield. This improvement is significant, with yields rising from
139 34.35% at 10 ppm to 85.58% at 30 ppm, reaching 95.39% at 50 ppm oxidant.

ACCEPTED MANUSCRIPT

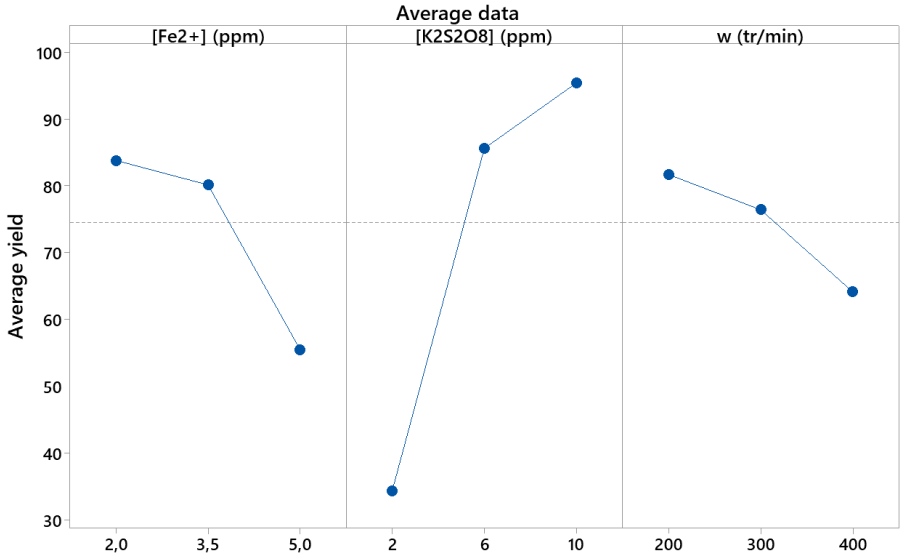

Figure 4. Main effects of the factors studied on the degradation yield of MG

Figure 5 shows the interaction effects on the degradation yield of Malachite Green. The strong interactions obtained between:

- At 6 ppm oxidant between 2 and 3.5ppm catalyst.
- At 250 rpm between 2 and 3.5 ppm of [Fe^{2+}].
- At 350 rpm between 2 and 3.5 ppm of [Fe^{2+}].
- At 300 rpm, between 6 and 10 ppm of oxidant.

Weak interactions are also observed between:

- At 10 ppm of oxidant between the three concentrations of [Fe^{2+}].
- At 200 rpm between 2 and 5ppm of [Fe^{2+}].
- At 200 rpm between 6 and 10ppm [$K_2S_2O_8$].

ACCEPTED MANUSCRIPT

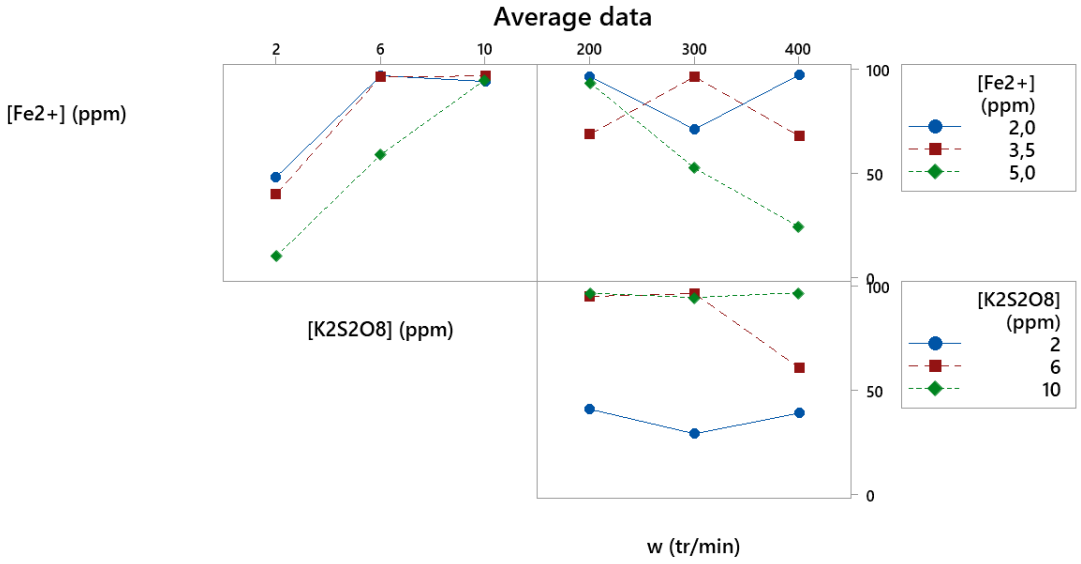

Figure 5. Interaction effects of the factors studied.

3.1.4. Pareto diagram

The Pareto diagram is used to evaluate the value and importance of effects. This diagram presents the absolute value of the effects of factors and includes a reference line on the graph. According to Figure 6, any effect that exceeds this reference line can be considered significant. The terms identified as significant are oxidant concentration [$K_2S_2O_8$], iron concentration [Fe^{2+}], the oxidant quadratic term ([$K_2S_2O_8$])², and the interaction between iron and stirring rate [Fe^{2+}]*w. This confirms the results obtained previously.

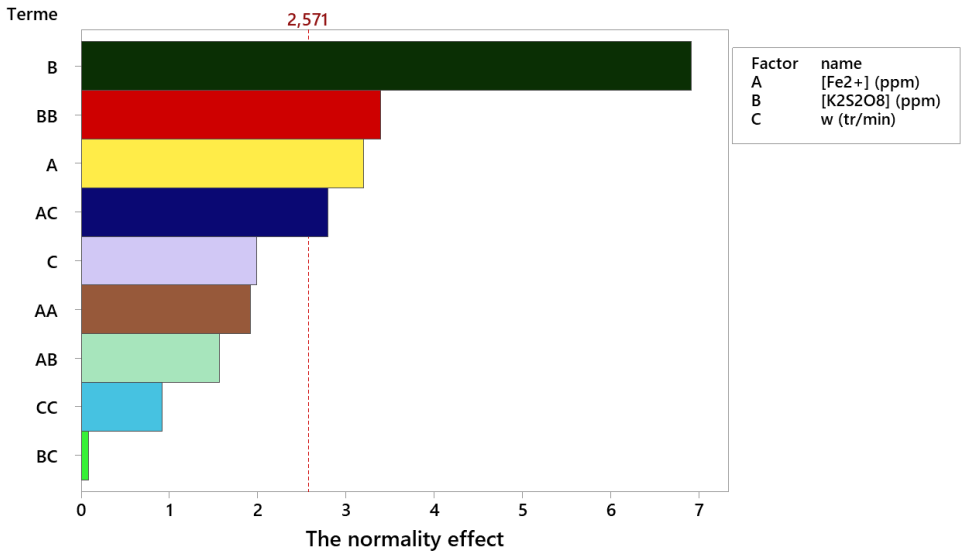

Figure 6. Pareto diagram for MG degradation

3.1.5. Mathematical model

The mathematical model is second-order and relates the degradation yield of MG to the various factors, their squares, and their interaction.

The regression of the response in coded units as a function of all terms is represented by equation 2, and in uncoded units by equation 3.

Regression equation in coded units

$$\boldsymbol{Y}\ (\%) = -147.4 + 54.6 \times [\boldsymbol{Fe^{2+}}] + 3.62 \times [\boldsymbol{K_2S_2O_8}] + 6.70 \times \boldsymbol{w} - 5.54 \times [\boldsymbol{Fe^{2+}}]^2 - 0.0551 \times [\boldsymbol{K_2S_2O_8}]^2 - 0.0597 \times \boldsymbol{w^2} + 0.325 \times [\boldsymbol{Fe^{2+}}] \times [\boldsymbol{K_2S_2O_8}] - 1.164 \times [\boldsymbol{Fe^{2+}}] \times w + 0.0026 \times [\boldsymbol{K_2S_2O_8} \times]w \quad (\mathbf{3})$$

Regression equation in uncoded units

$$\boldsymbol{Y}\ (\%) = 96.13 - 14.13 \times [\boldsymbol{Fe^{2+}}] + 30.52 \times [\boldsymbol{K_2S_2O_8}] - 8.76 \times w - 12.47 \times [\boldsymbol{Fe^{2+}}]^2 - 22.03 \times [\boldsymbol{K_2S_2O_8}]^2 - 5.97 \times \boldsymbol{w^2} + 9.76 \times [\boldsymbol{Fe^{2+}}] \times [\boldsymbol{K_2S_2O_8}] - 17.46 \times [\boldsymbol{Fe^{2+}}] \times w + 0.52 \times [\boldsymbol{K_2S_2O_8} \times]w \quad (\mathbf{4})$$

3.1.6. Response surfaces

Minitab18 allows us to plot response and contour surfaces by varying two factors simultaneously and setting the third at different levels (min, medium, and max). The surface and contour figures show that MG degradation yields are very good (around 100%). The zone of best yields is obtained at an oxidant concentration between 5.5-10ppm and throughout the range of Fe^{2+} concentration at a minimum level for the stirring speed (200rpm).

The response surface is concave and slightly inclined.

ACCEPTED MANUSCRIPT

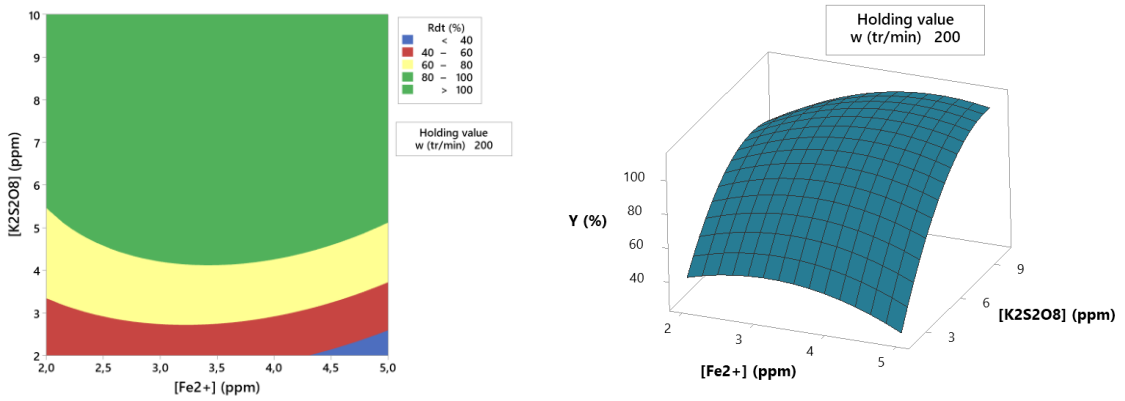

187 **Figure 7.** Contour and response surfaces of Y as a function of $[Fe^{2+}]$-$[K_2S_2O_8]$ at 200 rpm

188

189 Figure 8 shows MG degradation efficiency's response and contour surfaces by varying $[Fe^{2+}]$ and w

190 at 6 ppm for $[K_2S_2O_8]$.

191 It can be seen that total degradation of the pollutant was obtained, and the zone of good yields is

192 located in the middle of the chosen domain in inclined form (blue contour).

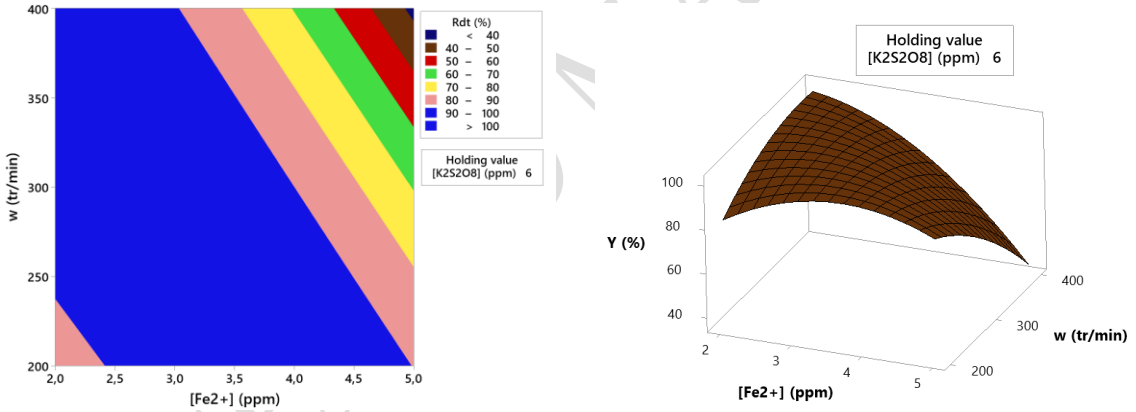

193 **Figure 8.** Contour and response surfaces of Y as a function of $[Fe^{2+}]$-w at 6ppm $[K_2S_2O_8]$

194 *3.1.7. Optimization*

195 The main objective was to identify the optimum operating conditions for achieving complete

196 degradation of MG. A constraint was imposed on the selected factors.

197 After several optimizations, the optimum conditions are summarized in Table 5. The results of these

198 optimizations were used to determine the ideal values for each factor influencing the process, as well

199 as the theoretical maximum value for malachite green (MG) degradation efficiency.

200

ACCEPTED MANUSCRIPT

Table 5. Optimization results for malachite green

Factors	$[Fe^{2+}]$ ppm	$[K_2S_2O_8]$ ppm	W rpm	Y_{th} (%)	d
Opt.	3.5	3.07	200	100	1,00

These results show that the optimum conditions for the complete degradation of MV are a $[Fe^{2+}]$ concentration of 3.5 ppm, a $[K_2S_2O_8]$ concentration of 3.07 ppm, and a stirring speed of 200 rpm. Under these conditions, a theoretical degradation yield of 100% was achieved.

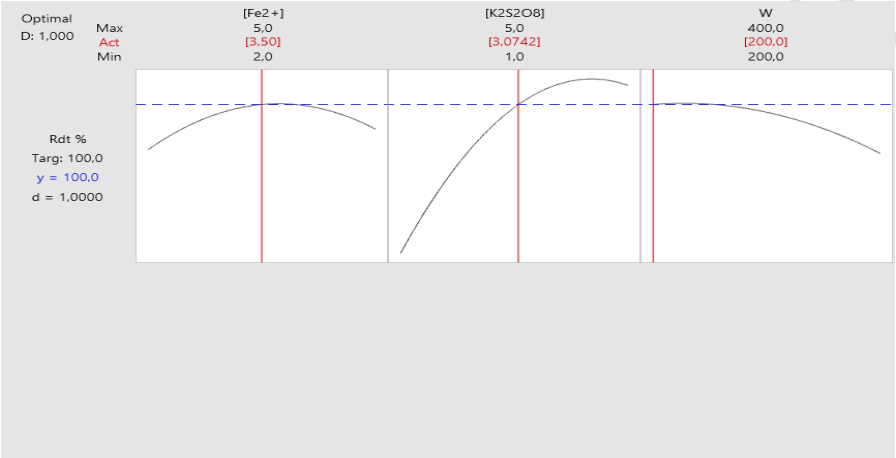

Figure 9. Optimization diagram for MG degradation

The theoretical model predicts a degradation efficiency of 100% for these optimized values. A verification test was carried out twice under the same experimental conditions to validate these optimum conditions. The experimental results showed an average yield of 98%, confirming the accuracy of the theoretical model. These results indicate that the model is adequate to represent the degradation process under the optimized conditions.

3.2. Discussion

Persulfate concentration $S_2O_4^{2-}$ plays a crucial role in the degradation system $S_2O_4^{2-}/Fe^{2+}$. The persulfate anion can be activated, either by thermal conditions or by chemical catalysts such as transition metal ions, to generate a powerful oxidant, the sulfate free radical ($SO_4^{\cdot-}$). This radical is extremely reactive and actively participates in the degradation of organic pollutants (Rastogi et al. 2008, Zhang et al. 2011, Li et al. 2014, Wang et al. 2017)

ACCEPTED MANUSCRIPT

The impact of free radicals and transition metal ions Fe^{2+} on the degradation process has been widely studied. An increase in persulfate concentration promotes the formation of additional sulfate radicals, accelerating the degradation rate of methyl green (MG). This observation is in line with previous studies, which show that higher persulfate concentrations lead to faster MG degradation (Sun et al. 2011, Ho et al. 2012, Yu et al. 2013).

In addition, sulfate radicals formed by persulfate activation can initiate complex chain reactions involving radical transfer. These reactions contribute to more efficient contaminant degradation. The dynamics of these chain reactions and their impact on degradation rates are influenced by persulfate concentration and the presence of transition metal ions, which modulate the production and consumption of free radicals (Yang et al. 2012, Li et al 2012, Kim et al. 2013).

The study also revealed that the presence of transition metal ions, such as iron, not only catalyzes the generation of sulfate radicals, but can also influence their stability and reactivity. The specific mechanisms by which these metal ions influence MG degradation merit further investigation to optimize reaction conditions and improve the efficiency of persulfate-based degradation systems (Lee et al. 2012, Ding et al. 2014, Liu et al. 2015).

The sulfate radicals formed by adding the catalyst can trigger a series of radical transfer chain reactions (Rastogi et al. 2009, Bennedsen et al. 2012, Fang et al.2023).

$$SO_4^{\cdot-} + H_2O \rightarrow HSO_4^- + OH$$

$$SO_4^{\cdot-} + Fe^{2+} \rightarrow SO_4^{2-} + Fe^{3+}$$

$$S_2O_4^{2-} + Fe^{2+} \rightarrow SO_4^{2-} + Fe^{3+} + SO_4^{\cdot-}$$

$$2SO_4^{\cdot-} \rightarrow S_2O_8^{2-}$$

3.3. Kinetics of malachite green degradation in a real matrix

In order to investigate the kinetics of malachite green degradation in different natural environments, various experiments were carried out at room temperature under a stirring speed of around 300 rpm for 1h. The physicochemical characteristics of the waters used are shown in Table 6. The concentrations are in ppm.

ACCEPTED MANUSCRIPT

Table 6: Characteristics of waters used

	Ca^{2+}	Mg^{2+}	K^{+}	Na^{+}	HCO_3^-	SO_4^{2-}	NO_3^-	NO_2^-	Cl^-	dry residue at180°C	pH
1	99	24	2.1	15.8	265	68	15	<0.02	72	380	7.20
2	72	27	2	11	336	11	20.20	<0.01	21	475	7.28
3	0.01	0.006	3.05	0.004	0.23	/	0.02	<0.01	0.23	1.51	6.20
4	430	1.45	400	12	160	3.1	2.00	<0.01	21	38	8.00

(1) natural mineral water (ifri); (2) Source water; (3) industrial water; (4) seawater.

It should be noted that the industrial water used in this study is desalinated water, intended for the cooling circuits of the Fertial complex, and was used as the actual matrix. In addition, the spring water used in this part of the work was collected from a mountain at Séraidi, near Annaba. This water was stored in a container at a temperature of 4°C.

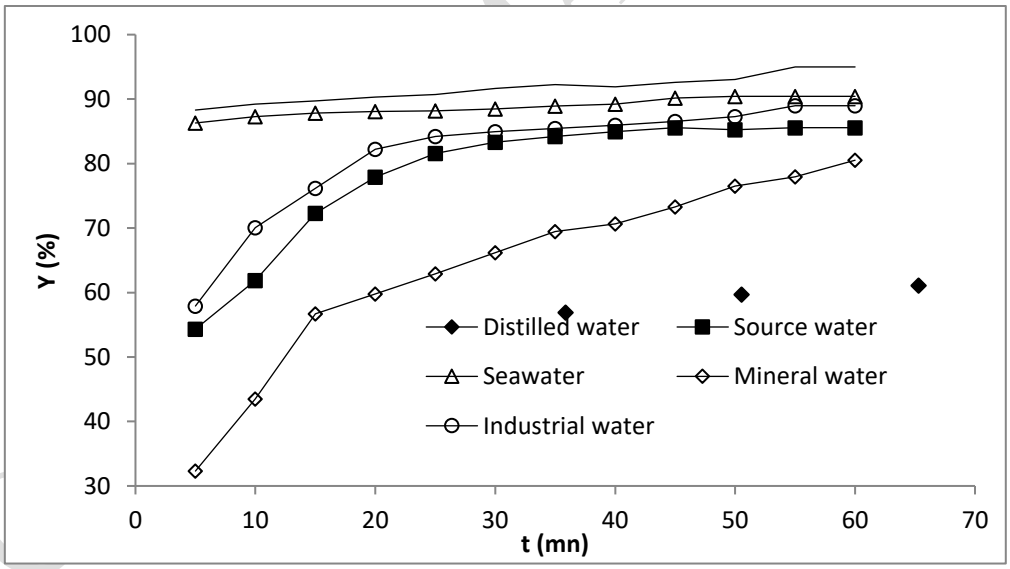

Figure 10. Effect of real matrix on degradation efficiency of malachite green

It was found that yields vary according to the physicochemical characteristics of each type of water. Distilled water, which is free of ions and impurities, allows a maximum degradation of 98% due to the absence of interference with sulfate radicals (Huang et al. 2020). In contrast, seawater and industrial water show similar efficiencies of 88.97%, due to their high concentration of chloride ions

ACCEPTED MANUSCRIPT

(Cl^-) and conductivity, which can influence the reactivity of sulfate radicals and alter the efficiency of the degradation process (Smith et al. 2018). Source water, with a yield of 85.57%, has high concentrations of bicarbonates and calcium, which can interact with the radicals or malachite green, reducing the rate of degradation (Johnson et al. 2019). Finally, natural mineral water, with the lowest yield of 80.52%, contains a high concentration of various ions, such as calcium and magnesium, as well as a significant dry residue, which can complex the radicals or neutralize their action (Williams et al. 2019). These variations can be explained by the influence of the specific physicochemical characteristics of each medium on the effectiveness of sulfate radicals in the degradation process of malachite green.

4. CONCLUSION

In order to eliminate malachite green from aqueous solutions, an advanced oxidation process was investigated. The experimental Box-Behnken design was used to determine the optimum operating conditions for improving the percentage of dye removal using a modified Fenton-like process. In fact, the three factors studied were: catalyst concentration [Fe^{2+}], oxidant concentration [$K_2S_2O_8$] and stirring speed. The results of the analysis of variance (ANOVA) showed that oxidant concentration [$K_2S_2O_8$] was the most significant parameter for malachite green degradation, with a probability value (p-value) of 0.001. In addition, catalyst concentration [Fe^{2+}], the oxidant quadratic term [$K_2S_2O_8$]², and the interaction between catalyst concentration and stirring speed [Fe^{2+}] * W were also identified as significant, with p-values of 0.024, 0.019 and 0.038 respectively.

Based on these results, the optimum conditions for malachite green removal were determined to be a catalyst concentration of 3.5 ppm, an oxidant concentration of 3.07 ppm, and a stirring speed of 200 rpm. These conditions enable a theoretical degradation yield of 100% to be achieved, while experimental tests showed a yield of 98%. This agreement confirms not only the effectiveness of the model used to represent the degradation process under the optimized conditions, but also that the parameters identified play a crucial role in the almost complete removal of the dye. Indeed, the

ACCEPTED MANUSCRIPT

experimental results show that the optimized conditions achieve a yield close to that predicted theoretically, thus validating the importance of the optimized parameters in the degradation process. Furthermore, in order to investigate the degradation kinetics of malachite green in different natural media, experiments were carried out at room temperature, with a stirring speed of 300 rpm for 1 hour. The results showed that malachite green oxidation follows the following order:

distilled water (98%) > seawater ≈ industrial water (88.97%) > source water (85.57%) > mineral water (80.52%).

Acknowledgments

We all are expressing our heartfelt gratitude to Badji Mokhtar-Annaba University for supporting research. We thank also the LOMOP Research Laboratory for providing us with the necessary material resources.

Conflict of Interest

The authors have no conflicts of interest to disclose

Funding

No funding was received.

References

Anipistakis, G. P., & Dionysiou, D. D. (2003). Degradation of organic contaminants in water with sulfate radicals generated by the conjunction of peroxymonosulfate with cobalt. Environmental Science & Technology, 37, 4790–4797.

Anipistakis, G. P., & Dionysiou, D. D. (2004). Transition metal/UV-based advanced oxidation technologies for water decontamination. Applied Catalysis B: Environmental, **54**, 155–163.

Azizpour, M., Ghaedi, H., Jalilzadeh Yengejeh, R., & Saberi, M. (2024). Performance Evaluation of the Photo-Fenton Process in the Removal of Vancomycin Antibiotic from Aqueous Solutions and Assessment of the Impact of Influential Parameters on the Process. *Iranian Journal of Chemistry and Chemical Engineering*. Article in press.

ACCEPTED MANUSCRIPT

Babaei, A. A., Ghanbari, F., & Jalilzadeh Yengejeh, R. (2017). Simultaneous use of iron and copper anodes in photoelectro-Fenton process: concurrent removals of dye and cadmium. *Water Science and Technology*, **75**(7), 1732–1742.

Baban, A., Yediler, A., & Ciliz, N. K. (2010). Integrated water management and CP implementation for wool and textile blend processes. Clean Technologies and Environmental Policy, **38**, 84–90.

Bahadir, K. K., & Abdurrahman, T. (2008). Electrochemical treatment of simulated textile wastewater with industrial components and Levafix Blue CA reactive dye: Optimization through response surface methodology. Journal of Hazardous Materials, **151**, 422–431.

Bendebane, F., Halaimia, F., Bahloul, L., Bouziane, L., & Ismail, F. (2016). Extraction of naphthalene in dynamic mode, application of Box-Behnken design. *Pollution Research, **35***(4), 23–29.

Bendebane, S., Bendebane, H., Bendebane, F., & Ismail, F. (2021). Sorption of methylene blue by luffa cylindrical: Optimization and modeling using the response surface methodology. *Algerian Journal of Engineering Research, **4***(2)

Bennedsen, L. R., Muff, J., & Sogaard, E. G. (2012). Influence of chloride and carbonates on the reactivity of activated persulfate. Chemosphere, **86**, 1092–1097.

Barati, G., Borghei, M., Jalilzadeh Yengejeh, R., & Takdastan, A. (2024). Investigating the performance of the photo-Fenton process of the Naphthalene removal from petroleum wastewater. *Iranian Journal of Chemistry and Chemical Engineering*. Article in press.

Ding, J. M., et al. (2014). Influence of transition metals on the generation of sulfate radicals in persulfate activation processes. Journal of Environmental Science, **26**(5), 1012–1020.

Fang, G., Gao, J., Dionysiou, D. D., Liu, C., & Zhou, D. (2023). Activation of persulfate by quinones: Free radical reactions and implications for the degradation of PCBs. *Environmental Science & Technology*, 47(9), 4605–4611.

ACCEPTED MANUSCRIPT

Forgacs, E., Cserhati, T., & Oros, G. (2004). Removal of synthetic dyes from wastewaters: A review. Environment International, 30, 953–971.

Gashtasbi, F., Jalilzadeh Yengejeh, R., & Babaei, A. A. (2017). Adsorption of vancomycin antibiotic from aqueous solution using an activated carbon impregnated magnetite composite. *Desalination and Water Treatment*, **88**, 286–297.

Ghodbane, H., Nikiforov, A. Y., Hamdaoui, O., Surmont, P., Lynen, F., & Willems, G. (2014). Non-thermal plasma degradation of anthraquinonic dye in water: Oxidation pathways and effect of natural matrices. Journal of Advanced Oxidation Technologies, 17, 372–384.

Gupta, V. K., & Suhas. (2009). Application of low-cost adsorbents for dye removal – A review. Journal of Environmental Management, 90, 2313–2342.

Ho, M. P., et al. (2012). Persulfate oxidation of organic contaminants in aqueous solutions. Environmental Chemistry Letters, 10(4), 527–534

Huang, Y., Chen, X., & Liu, Y. (2020). Effects of water quality on the degradation efficiency of organic pollutants. Journal of Environmental Sciences, 45, 123–134

Ivanov, K. L., Glebov, E. M., Plyusnin, V. F., Ivanov, Y. V., Grivin, V. P., & Bazhin, N. M. (2000). Laser flash photolysis of sodium persulfate in aqueous solution with additions of dimethylformamide. Journal of Photochemistry and Photobiology A: Chemistry, **133**, 99–104.

Jalilzadeh Yengejeh, R., Sekhavatjou, M. S., Maktabi, P., Arbab Soleimani, N., Khadivi, S., & Pourjafarian, V. (2014). The Biodegradation of Crude Oil by *Bacillus subtilis* Isolated from Contaminated Soil in Hot Weather Areas. *International Journal of Environmental Research*, **8**(2), 509–514.

Jiraratananon, R., Sungpet, A., & Luangsowan, P. (2000). Performance evaluation of nanofiltration membranes for treatment of effluents containing reactive dye and salt. Desalination, **130**, 177–183.

ACCEPTED MANUSCRIPT

Johnson, M., Lee, K., & Patel, A. (2019). Influence of bicarbonates and calcium on oxidative degradation. Chemical Engineering Journal, **359**, 1124–1133.

Karimipour, Z., Jalilzadeh Yengejeh, R., Haghighatzadeh, A., Mohammadi, M. K., & Mohammadi Rouzbehani, M. (2021). UV-Induced Photodegradation of 2,4,6-Trichlorophenol Using Ag–Fe2O3–CeO2 Photocatalysts. *Journal of Inorganic and Organometallic Polymers and Materials*, **31**, 1143–1152.

Kim, Y. M., et al. (2013). Mechanism and kinetics of sulfate radical-mediated oxidation of organic contaminants. Applied Catalysis B: Environmental, **135**, 297–304.

Koyuncu, I. (2002). Reactive dye removal in dyes/salt mixtures by nanofiltration membranes containing vinylsulphone dyes: Effects of feed concentration and cross-flow velocity. Desalination, **143**, 243–253.

Lee, C. H., et al. (2012). The catalytic role of transition metals in sulfate radical-based advanced oxidation processes. Chemical Engineering Journal, **198**, 385–394.

Lee, J. W., Choi, S. P., Thiruvenkatachari, R., Shim, W. G., & Moon, H. (2006). Evaluation of the performance of adsorption and coagulation processes for the maximum removal of reactive dyes. Dyes and Pigments, **69**, 196–203.

Li, H., et al. (2014). Sulfate radical-based advanced oxidation processes for environmental remediation. Environmental Science and Pollution Research, **21**(5), 3432–3441.

Li, Q. Z., et al. (2012). Role of sulfate radicals in the degradation of organic pollutants. Chemical Engineering Journal, 195-196, 1–12.

Liang, C. J., Bruell, C. J., Marley, M. C., & Sperry, K. L. (2003). Thermally activated persulfate oxidation of trichloroethylene (TCE) and 1,1,1-trichloroethane (TCA) in aqueous systems and soil slurries. Soil and Sediment Contamination, **12**, 207–228.

ACCEPTED MANUSCRIPT

Liang, C., & Bruell, C. J. (2008). Thermally activated persulfate oxidation of trichloroethylene: Experimental investigation of reaction orders. Industrial & Engineering Chemistry Research, 47(9), 2912–2918

Liu, H. L., & Chiou, Y. R. (2006). Optimal decolorization rate of Reactive Red 239 by UV/ZnO photocatalytic process. Journal of the Chinese Institute of Chemical Engineers, **37**, 289–298.

Liu, L. J., et al. (2015). Optimizing the conditions for persulfate-based degradation of contaminants using metal ion catalysis. Environmental Science & Technology, **49**(14), 8425–8433.

Nemati, N., Jorfi, S., Jalilzadeh Yengejeh, R., Mohammadiroozbahani, M., & Sabzalipour, S. (2024). Efficiency of an Advanced Sono-Photo Electro Kinetic Process in the Removal of Furfural from the Saline Effluent of a Refinery Using Titanium Dioxide Nanoparticles (TiO_2). *Iranian Journal of Chemistry and Chemical Engineering*. Article in press.

Rai, H. S., Bhattacharyya, M. S., Singh, J., Bansal, T. K., Vats, P., & Banerjee, U. C. (2005). Removal of dyes from the effluent of textile and dyestuff manufacturing industry: A review of emerging techniques with reference to biological treatment. Critical Reviews in Environmental Science and Technology, **35**, 219–238.

Rangabhashiyam, S., Anu, N., & Selvaraju, N. (2013). Sequestration of dye from textile industry wastewater using agricultural waste products as adsorbents. Journal of Environmental Chemical Engineering, **1**, 629–641.

Rastogi, A., Al-Abed, S. R., & Dionysiou, D. D. (2009). Sulfate radical-based ferrous–peroxymonosulfate oxidative system for PCBs degradation in aqueous and sediment systems. Applied Catalysis B: Environmental, 85, 171–179.

Rastogi, K., Sahu, J. N., Meikap, B. C., & Biswas, M. N. (2008). Hazardous materials removal using advanced oxidation processes. Journal of Hazardous Materials, **151**, 422–431.

ACCEPTED MANUSCRIPT

Shobirynia, M., Jalilzadeh Yengejeh, R., Derikvand, E., & Mohammadi Rouzbahani, M. (2024). Comparison of Electro-Fenton and Photoelectro-Fenton for Removal of Acrylonitrile Butadiene Styrene (ABS) from Petrochemical Wastewater. *Iranian Journal of Chemistry and Chemical Engineering*, 133–144.

Shokri, R., Jalilzadeh Yengejeh, R., Babaei, A. A., Derikvand, E., & Almasi, A. (2020). Advanced Oxidation Process Efficiently Removes Ampicillin from Aqueous Solutions. *Iranian Journal of Toxicology*, **14**(2), 123–130.

Smith, R., Wang, J., & Brown, T. (2018). Impact of chloride concentrations on oxidation processes. Environmental Chemistry Letters, **16**, 789–798.

Soloman, P. A., Basha, C. A., Ramamurthi, V., Koteeswaran, K., & Balasubramanian, N. (2009). Electrochemical degradation of Remazol Black B dye effluent. Clean Technologies and Environmental Policy, 37, 889–900

Souhaimi, K., Zahrim, A. Y., & Hilal, N. (2011). Modelling and optimization of coagulation of highly concentrated industrial grade leather dye by response surface methodology. Chemical Engineering Journal, **167**, 77–83.

Sun, A. L., et al. (2011). Influence of persulfate concentration on the degradation rate of organic pollutants. Water Research, **45**(7), 2349–2356.

Wang, V. C., et al. (2017). Persulfate activation for advanced oxidation processes: A review. Journal of Environmental Management, **204**, 491–504.

Williams, S., Martinez, A., & Lopez, R. (2019). Effect of ion concentration on the efficiency of radicals in water treatment. Water Research, **158**, 84–93.

Wu, H., Yang, R., Li, R., Long, C., Yang, H., & Li, A. (2015). Modeling and optimization of the flocculation processes for removal of cationic and anionic dyes from water by an amphoteric

ACCEPTED MANUSCRIPT

grafting chitosan-based flocculant using response surface methodology. Environmental Science and Pollution Research.

Yang, R. Y., et al. (2012). Degradation of organic contaminants by persulfate activation with Fe(II): Kinetics and mechanisms. Journal of Hazardous Materials, 237-238, 327–334.

Yu, J. K., et al. (2013). Efficient removal of methylene blue dye by persulfate-based oxidation. Chemical Engineering Journal, **221**, 261–269.

Zahrim, A. Y., & Hilal, N. (2013). Treatment of highly concentrated dye solution by coagulation/flocculation–sand filtration and nanofiltration. Water Resources and Industry, 3, 23–34.

Zhang, Y. J., et al. (2011). Degradation of organic contaminants using persulfate activated by transition metal ions. Environmental Science & Technology, 45(14), 6145–6152.

Zhao, D., Liao, X., Yan, X., & Chen, Y. (2013). Persulfate activation for the degradation of organic pollutants: Advances in fundamental and applied research. Chemical Engineering Journal, **223**, 492–501.

Zonoozi, M. H., Moghaddam, M. R., & Arami, M. (2009). Coagulation/flocculation of dye-containing solutions using polyaluminium chloride and alum. Water Science and Technology, **59**, 1343–1351.

ACCEPTED MANUSCRIPT